

2013

## AGENT BASED, DISTRIBUTED CONTROL STRATEGIES AND OPTIMIZATION OF PLUG-IN ELECTRIC VEHICLES ON SMART/ MICROGRID ARCHITECTURES

Kyle Bordeau  
*Michigan Technological University*

Follow this and additional works at: <https://digitalcommons.mtu.edu/etds>



Part of the [Mechanical Engineering Commons](#)

Copyright 2013 Kyle Bordeau

---

### Recommended Citation

Bordeau, Kyle, "AGENT BASED, DISTRIBUTED CONTROL STRATEGIES AND OPTIMIZATION OF PLUG-IN ELECTRIC VEHICLES ON SMART/MICROGRID ARCHITECTURES", Master's Thesis, Michigan Technological University, 2013.

<https://doi.org/10.37099/mtu.dc.etds/629>

Follow this and additional works at: <https://digitalcommons.mtu.edu/etds>



Part of the [Mechanical Engineering Commons](#)

AGENT BASED, DISTRIBUTED CONTROL STRATEGIES AND OPTIMIZATION OF  
PLUG-IN ELECTRIC VEHICLES ON SMART/MICROGRID ARCHITECTURES

By

Kyle D. Bordeau

A THESIS

Submitted in partial fulfillment of the requirements for the degree of

MASTER OF SCIENCE

In Mechanical Engineering

MICHIGAN TECHNOLOGICAL UNIVERSITY

2013

© 2013 Kyle D. Bordeau

This thesis has been approved in partial fulfillment of the requirements for the Degree of  
MASTER OF SCIENCE in Mechanical Engineering.

Department of Mechanical Engineering - Engineering Mechanics

Thesis Advisor: *Dr. Gordon Parker*

Committee Member: *Dr. Rush Robinett*

Committee Member: *Dr. Allan Struthers*

Department Chair: *Dr. William Predebon*

## **Dedication**

To all of the victims of the 2013 Boston Marathon bombings and their families, and to all others that were affected and those that provided help and support. I thank god for the safety of my brother, Rick, and his wife, Michelle. "It was a good day to have a bad day,"

April 15, 2013.

# Contents

|   |            |
|---|------------|
| <b>List of Figures</b> . . . . .                      | <b>vii</b> |
| <b>List of Tables</b> . . . . .                       | <b>ix</b>  |
| <b>Preface</b> . . . . .                              | <b>x</b>   |
| <b>Acknowledgments</b> . . . . .                      | <b>xi</b>  |
| <b>Abstract</b> . . . . .                             | <b>xii</b> |
| <b>1 Introduction and Literature Review</b> . . . . . | <b>1</b>   |
| 1.1 Power Grids . . . . .                             | 1          |
| 1.1.1 Smart Grid . . . . .                            | 2          |
| 1.1.2 Microgrids . . . . .                            | 3          |
| 1.2 Plug-In Electric Vehicles . . . . .               | 4          |
| 1.2.1 PEV Charging Strategies . . . . .               | 5          |
| 1.2.1.1 Time of Use Control . . . . .                 | 5          |
| 1.2.1.2 Centralized Control . . . . .                 | 6          |
| 1.2.1.3 Distributed Control . . . . .                 | 6          |

|          |   |           |
|----------|---|-----------|
| <b>2</b> | <b>Microgrid Component Optimal Sizing</b> | <b>8</b>  |
| 2.1      | Introduction                              | 8         |
| 2.2      | Methodology                               | 10        |
| 2.2.1    | Model Description                         | 10        |
| 2.2.2    | Analysis                                  | 15        |
| 2.3      | Results                                   | 18        |
| 2.4      | Conclusions                               | 19        |
| <b>3</b> | <b>Distributed Smart Charge Control</b>   | <b>22</b> |
| 3.1      | Introduction                              | 22        |
| 3.2      | Methodology                               | 23        |
| 3.2.1    | Model Description                         | 23        |
| 3.2.2    | Analysis                                  | 27        |
| 3.3      | Results                                   | 28        |
| 3.4      | Conclusions                               | 33        |
| <b>4</b> | <b>Discussion</b>                         | <b>35</b> |
| 4.1      | Summary                                   | 35        |
| 4.2      | Future Work                               | 37        |
|          | <b>References</b>                         | <b>40</b> |
| <b>A</b> | <b>MATLAB Code</b>                        | <b>45</b> |
| A.1      | Microgrid Component Optimal Sizing Code   | 46        |

|          |   |           |
|----------|---|-----------|
| A.1.1    | Setup Script . . . . .                          | 46        |
| A.1.2    | Optimization Function . . . . .                 | 49        |
| A.1.3    | Grid Simulation Function . . . . .              | 50        |
| A.2      | Distributed Smart Charge Control Code . . . . . | 54        |
| A.2.1    | Setup Script . . . . .                          | 54        |
| A.2.2    | Grid Simulation Function . . . . .              | 57        |
| A.2.3    | Charge Control Functions . . . . .              | 59        |
| A.2.3.1  | Charge Control A . . . . .                      | 59        |
| A.2.3.2  | Charge Control B . . . . .                      | 60        |
| A.2.3.3  | Charge Control C . . . . .                      | 60        |
| <b>B</b> | <b>Letters of Permission . . . . .</b>          | <b>62</b> |
| B.1      | Chapter 2 Permission . . . . .                  | 62        |
| B.2      | Chapter 3 Permission . . . . .                  | 63        |

# List of Figures

|     |  |    |
|-----|--|----|
| 2.1 | Primary load profile, fixed throughout study . . . . .   | 11 |
| 2.2 | Primary load profile, fixed throughout study . . . . .   | 12 |
| 2.3 | Primary load profile, fixed throughout study . . . . .   | 12 |
| 2.4 | Simulation flow chart . . . . .  | 14 |
| 2.5 | Storage and NTV fleet energy states for a 20-vehicle grid, not optimized . .   | 16 |
| 2.6 | Storage and NTV fleet energy states for optimized 20-vehicle grid . . . . .  | 17 |
| 2.7 | Optimized simulation parameters normalized to the 20-vehicle grid solution   | 19 |
| 2.8 | Missed energy time in optimized grids for 50% loss in PV output<br>normalized to 20-vehicle grid solution, missed time is 36,476 second for<br>20-vehicle case . . . . . | 20 |
| 2.9 | Vehicle fleet final energy state with 50% PV output . . . . .  | 20 |
| 3.1 | Simulation flow chart . . . . .  | 25 |
| 3.2 | Load profile for 24-hour period with and without PEV load and no charge<br>control used . . . . .  | 26 |
| 3.3 | Load profile for 24-hour time period with and without PEV load using<br>Charge Control B, $\alpha_w = 3$ . . . . .   | 29 |

|     |  |    |
|-----|--|----|
| 3.4 | Load profile for 24-hour time period with and without PEV load using Charge Control B . . . . .              | 31 |
| 3.5 | Load profile for 24-hour time period with and without PEV load using Charge Control C . . . . .              | 32 |
| 3.6 | Load profile for 6-day time period with and without PEV load using no control and Charge Control C . . . . . | 34 |

# List of Tables

2.1 Simulation Parameters . . . . . 13

2.2 Optimized simulation parameters . . . . . 18

## **Preface**

Chapter 2 is republished material from a conference article that was presented at the Ground Vehicle Systems Engineering and Technology Symposium 2011 with minor changes and additions to adequately fit this text[1]. For the work presented, I performed all analyses and wrote the document. Co-authors provided technical input as well as assisted in editing the final submission.

Chapter 3 is republished material from a conference article that was presented at the IEEE International Symposium on Power Electronics, Electric Drives, Automation and Motion 2012 with minor changes and additions to adequately fit this text[2]. For the work presented, I performed all analyses and wrote the document. Co-authors provided technical input as well as assisted in editing the final submission.

Permissions to use this material is presented in Appendix B.

## Acknowledgments

First and foremost I would like to thank my advisor, Dr. Gordon Parker, for all of his help and encouragement during my time in grad school and even prior to that. Without his support none of this would have been possible.

I would also like to thank all others for the help they have contributed to my work both big and small: Matt Heath, Jack Kelly, Dr. Allan Struthers, and anyone else I may have forgotten. For providing the immensely helpful L<sup>A</sup>T<sub>E</sub>X templates that created this document, I need to recognize G for making this final process for my degree much easier than it otherwise could have been.

I want to thank all of my friends at Michigan Tech and in the Houghton area who have made the last 6 years here some of the most enjoyable in my life. I will always love this place.

Finally, I need to thank my family for all of the love and support that they've given me not only in college but throughout my entire life. Mom, Dad, Rick, and Molly, I love you all so much.

## **Abstract**

This thesis will present strategies for the use of plug-in electric vehicles on smart and microgrids. MATLAB is used as the design tool for all models and simulations.

First, a scenario will be explored using the dispatchable loads of electric vehicles to stabilize a microgrid with a high penetration of renewable power generation. Grid components for a microgrid with 50% photovoltaic solar production will be sized through an optimization routine to maintain storage system, load, and vehicle states over a 24-hour period. The findings of this portion are that the dispatchable loads can be used to guard against unpredictable losses in renewable generation output.

Second, the use of distributed control strategies for the charging of electric vehicles utilizing an agent-based approach on a smart grid will be studied. The vehicles are regarded as additional loads to a primary forecasted load and use information transfer with the grid to make their charging decisions. Three lightweight control strategies and their effects on the power grid will be presented. The findings are that the charging behavior and peak loads on the grid can be reduced through the use of distributed control strategies.

# **Chapter 1**

## **Introduction and Literature Review**

### **1.1 Power Grids**

There are three main components to an electric power system: generation plants to produce electricity, transmission lines to carry electricity, and transformers to alter voltage. There are a number of fuels that the generation plants can use to produce the electricity such as coal, nuclear, or solar. Fuel flexibility allows plants to be located just about anywhere. The existing power grid has been pieced together as isolated regions have required power and built independent utilities that would later be tied together[3]. In North America there are over one million kilometers of transmission lines[4] that are governed by only three major interconnections[3]. While the current state of the power grid is much more

organized than it once was it “is aging, inefficient, and congested, and incapable of meeting the future energy needs of the Information Economy without operational changes and substantial capital investment over the next several decades[5].” Two alternatives to the current electric power system that have been proposed and are being researched are smart grids and microgrids.

### **1.1.1 Smart Grid**

A document released by the U.S. Department of Energy in 2003, “*Grid 2030*” *A National Vision for Electricity’s Second 100 Years*, discusses the necessary changes to the current infrastructure. It calls for new superconducting materials that will virtually eliminate transmission losses, distributed intelligence to facilitate two-way flow of electricity and information, and distributed energy sources all in an effort to increase the efficiency and quality of the nation’s power grid[5]. This idea is commonly referred to as a smart grid, and it represents a completely different architecture that can make use of the significant accomplishments in information technology. The smart grid will be more reliable, more secure, more economical, more efficient, more environmentally friendly, and safer[6].

While many of these characteristics will be facilitated by new hardware with updated materials, the capability of information transfer enables the limits of the smart grid’s capabilities to really be pushed. The power electronic interface that can be incorporated

into many devices that are connected to the grid such as appliances or electric vehicles provide infinite control options to users and utilities to tune the grid's operation[7]. These individual electronics act as 'agents' on the grid and can communicate information with a centralized grid entity or other agents. This allows for any local operating condition to be relayed throughout the grid.

### **1.1.2 Microgrids**

Dr. Robert Lasseter of the University of Wisconsin-Madison College of Engineering described microgrids as a "cluster of loads and micro sources operating as a single controllable system that provides both power and heat to its local area[8]." This a completely different way of thinking about how power is generated and utilized. Instead of isolated large generation plants, the demands on a microgrid are supported by multiple microsources that can be configured in any desired array. Significant power electronics are needed to control power flow in such an architecture, but it can be achieved through the use of local microsource controllers, a system optimizer, and distributed protection[8]. Microgrids can operate in isolation or as a part of a larger macrogrid.

Microgrids provide significant benefits when compared to a conventional power grid. Among these benefits is the ability to provide higher local reliability. This is accomplished through "islanding" where the microgrid is cut off from external fluctuations or problems

in the macrogrid[9]. During the tsunami that struck Japan in 2011, the port city of Sendai experienced massive outages as their electric grid was disabled, with the exception of Tohoku Fukushi University where an experimental microgrid was islanded from the macrogrid to sustain power and also provide heat[10].

Another microgrid benefit is improved efficiency. Existing power plants have an overall fuel-to-electricity efficiency of 28-32%[9]. In a microgrid, the relative proximity of generators means that the waste heat can be utilized locally and can increase the overall fuel-to-useful energy efficiency to over 80%.

A microgrid does not have to be one piece of a larger smart grid, they are also beneficial in their ability to operate independently. With no reliance on an interconnection with some distant generation source, microgrids can be assembled in virtually any location. This is useful in many applications, one of which would be in developing countries. In a place where time and money may be scarce, a microgrid infrastructure is much less expensive and faster to build than a large-scale grid[11].

## **1.2 Plug-In Electric Vehicles**

There is significant uncertainty surrounding the electrification of automobiles in the form of plug-in electric vehicles (PEVs), which includes both dedicated electric vehicles and

plug-in hybrid electric vehicles. Their adoption rate and specific utilization is unknown as well as the exact impact that their additional power demands will have on an already unstable power grid. A great deal of work has been done in an effort to predict the grid effects of PEV adoption, and also in the topic of controlling the behavior of these grids and vehicles.

### **1.2.1 PEV Charging Strategies**

Uncontrolled PEV charging puts stress on the grid such as voltage sag and line overloads[12]. Utilizing a control strategy for PEV charging could help to alleviate these problems. There are many different strategies for controlling the charging cycles of PEVs including time of use control, centralized control, and distributed control.

#### **1.2.1.1 Time of Use Control**

Time of use (TOU) control determines charging based on the time of day at which the vehicle is being used. Rashid Waraich performed a study using dual tariff charging, which is a type of time of use. This method utilizes higher charging costs during the day to discourage charging during the times of higher demand[13]. In this iterative process, charging times were found that would allow PEVs to charge for the lowest cost while still being able to make all required trips. This could be an effective method, but it is however a

complex procedure that works well for only predetermined scenarios. This method would also increase the maximum vehicle demand, when compared to uncontrolled charging, but during times of lower overall demand.

### **1.2.1.2 Centralized Control**

Centralized control strategies employ smart charging techniques. The smart grid provides a centralized agent, supervisor, that makes all decisions on charging. Waraich also implemented one such strategy. The vehicle, or user, inputs planned activities and the supervisor determines for all vehicles when they should be charging. This was implemented as an iterative approach[13], but could also be used otherwise with a complex scheduling algorithm. A University of Louisville case study provides another example of centralized control using forecasted demand[14]. The algorithm used determines the available charging capacity using the difference between the maximum demand for a period and the forecasted demand for the next 15-minute interval. The charging capacity is then used by the supervisor to determine vehicle charging habits.

### **1.2.1.3 Distributed Control**

Distributed controls are also smart charging techniques, but have no need for a supervisory controller. Because of this, individual agents have their own autonomy. Reiner introduces

a distributed control function that requires the user to input an approximate departure time when the vehicle is connected to the grid[12]. Vehicles calculate the amount of time it would take to fully charge the battery and then use this value to vie for a fixed number of charging slots. The vehicles that need the most time to charge have the highest priority. This method proves to decrease peak demands and spread out charging in simulation. This experiment however only models the vehicle charge load and not the overall grid load, so its overall effectiveness is unknown.

# Chapter 2

## Microgrid Component Optimal Sizing

### 2.1 Introduction

The U.S. DoD has a particular interest in decreasing fossil fuel usage and dependence on civilian energy sources at military installations. Renewable energy sources help to ease the supply line for a forward operating base (FOB) by decreasing fossil fuel consumption used for power generation and also provide silent generation capability in the case of solar energy. Electrification of U.S. Army non-tactical vehicles (NTVs) could impact the effectiveness of military base microgrids. This impact could be positive or negative depending on the level of upfront design implemented to ensure efficient and

---

The material contained in this chapter, including all figures and tables, was previously published as a conference article at the Ground Vehicle Systems Engineering and Technology Symposium 2011 with minor changes and additions to adequately fit this text[1].

harmonious integration of technologies. For example, renewable power sources tend to destabilize microgrids at high penetration levels [15] due to disturbances in sunlight or variable winds. Similarly, renewable sources such as solar and wind power suffer from being non-dispatchable, meaning they cannot be simply turned on or off like a diesel generator. However, the destabilizing effects of renewable sources can be overcome by using distributed energy resources, in the form of NTV fleets, through scheduling of charging loads and potential vehicle-to-grid source capability [16, 17].

Analysis and design tools are needed to optimize the charging and discharging of electric vehicles and the sizing of a traditional energy storage system in an effort to stabilize the power demands in a microgrid with high penetration renewable sources. The work presented in this chapter uses an example to illustrate possible effects that an electrified NTV fleet can have on a microgrid with 50% renewable generation.

An idealized microgrid, consisting of both photovoltaic (PV) and fixed generation power sources, energy storage, primary loads, and an NTV fleet is designed for several different NTV fleet sizes. For each optimal design, the effect of reducing the expected PV power output by 50% is calculated in terms of the amount of time the primary loads are missed and the state of charge of the NTV fleet. As the NTV fleet size increases, the effect of a 50% reduction in PV generation on primary load satisfaction is decreased. The per vehicle state of charge of the NTV fleet also decreases. This allows the calculation of the excess vehicle capacity needed in order to meet both fleet state of charge requirements and primary

load satisfaction in the presence of reduced PV generation.

## 2.2 Methodology

### 2.2.1 Model Description

This work focuses on how the design of a microgrid changes performance in response to an NTV fleet and forecasted PV generation when PV penetration is fixed at 50%. The microgrid and operational scenario descriptions are thus divided into features that are fixed for each scenario and features that are variable during the design.

The fixed aspects for each design scenario are the primary, or non-NTV, loads, shown in Figure 2.1, the shape of the source profile, shown in Figure 2.2, and the schedule when the NTV fleet is plugged into the grid, shown in Figure 2.3. The primary load has a constant power component at  $P_{fix} = 20kW$  and a varying component that ramps up between 0600 and 0700 as the base becomes ready for the day. It then holds constant at 60 kW and ramps back down between 1600 and 2400 to  $P_{fix}$  for the night. The source is a combination of constant generation (e.g. diesel genset) and PV generation. The PV profile ramps up between 0600 and 1100, holds constant for one hour, and then ramps down between 1300 and 1700, roughly mimicking the cycle of the sun. The entire NTV fleet operates on the same schedule and is plugged into the grid between 1100 and 1300 and between 1800 and

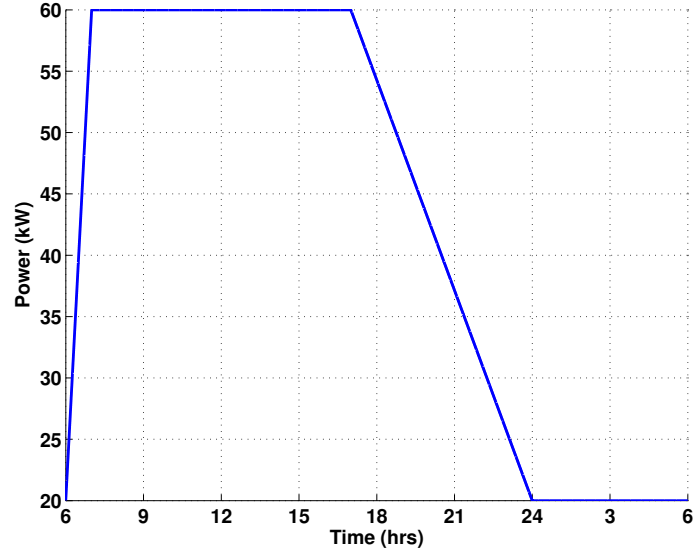


**Figure 2.1:** Primary load profile, fixed throughout study

0600. While plugged in, the fleet has the ability to draw up to  $P_{VehIn} = 1.1kW$  per vehicle. Whenever they are not plugged in, the vehicles are being used and discharge at the same rate as they charge,  $P_{VehOut} = P_{VehIn}$ .

The variable aspects of the model include the size of the PV array. Because PV penetration is fixed at 50% of the total generation, the PV size also affects the constant generation. Thus the overall source output can be described by one variable which is the maximum output of the PV array,  $P_{PVmax}$ , and scales the entire source profile. The other variables are the size of the energy storage system,  $E_{stormax}$ , and its initial state of charge at the beginning of the day,  $E_{storinit}$ . These three variable features will also make up the optimization parameters.

A set of parameters, an example of which is shown in Table 2.1, uniquely defines a microgrid design and its operational scenario. The system can be modeled with two states,  $E_{stor}$  and  $E_{NTV}$ , which are the storage system and NTV fleet states of charge respectively

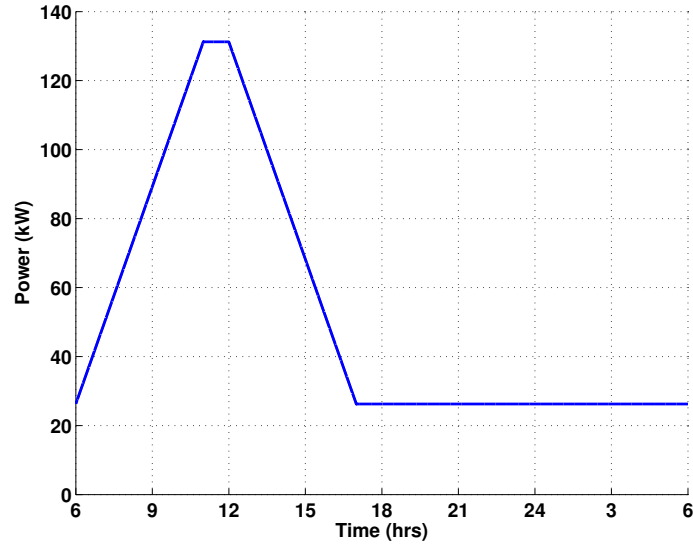


**Figure 2.2:** Primary load profile, fixed throughout study

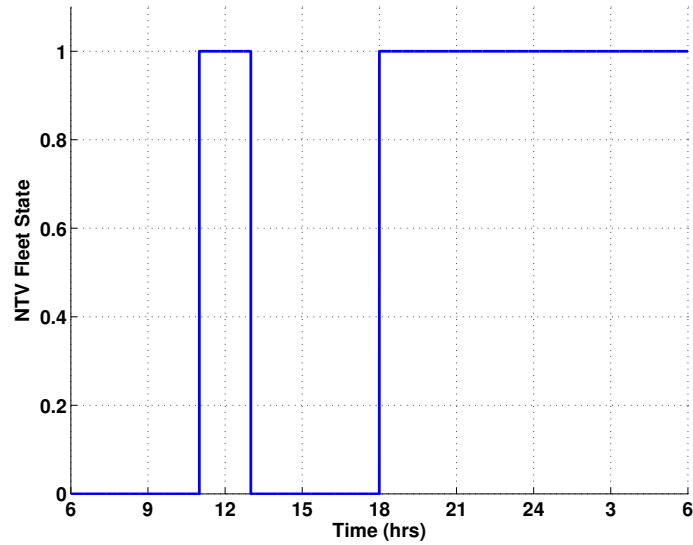


**Figure 2.3:** Primary load profile, fixed throughout study

shown in Eq. 2.1 and 2.2. A simulation was constructed in MATLAB to solve

**Table 2.1**  
Simulation Parameters

|                    |          |
|--------------------|----------|
| Fleet Size         | 20       |
| $P_{PVmax}$ (W)    | 1.00E+05 |
| $E_{stormax}$ (J)  | 8.07E+08 |
| $E_{storinit}$ (J) | 2.21E+07 |

$$\dot{E}_{stor} = P_{stornet} \tag{2.1}$$

$$\dot{E}_{NTV} = P_{NTVnet} \tag{2.2}$$

where  $P_{stornet}$  and  $P_{NTVnet}$  are nonlinear functions that are dependent on several factors, including available energy and vehicle plug-in state. The simulation uses Euler integration with a one second time step for a 24 hour period. A flowchart describing the control flow is shown in Figure 2.4.

The simulation first determines if excess power is available on the grid after satisfying the primary loads of Figure 2.1 using any combination of the PV, constant source, or the storage system. If there is not enough source power, then the mismatched load is computed. If there is excess source and stored energy, and the NTV fleet is plugged in, then the NTV fleet will charge if necessary. After charging the NTV fleet, any excess power is used to

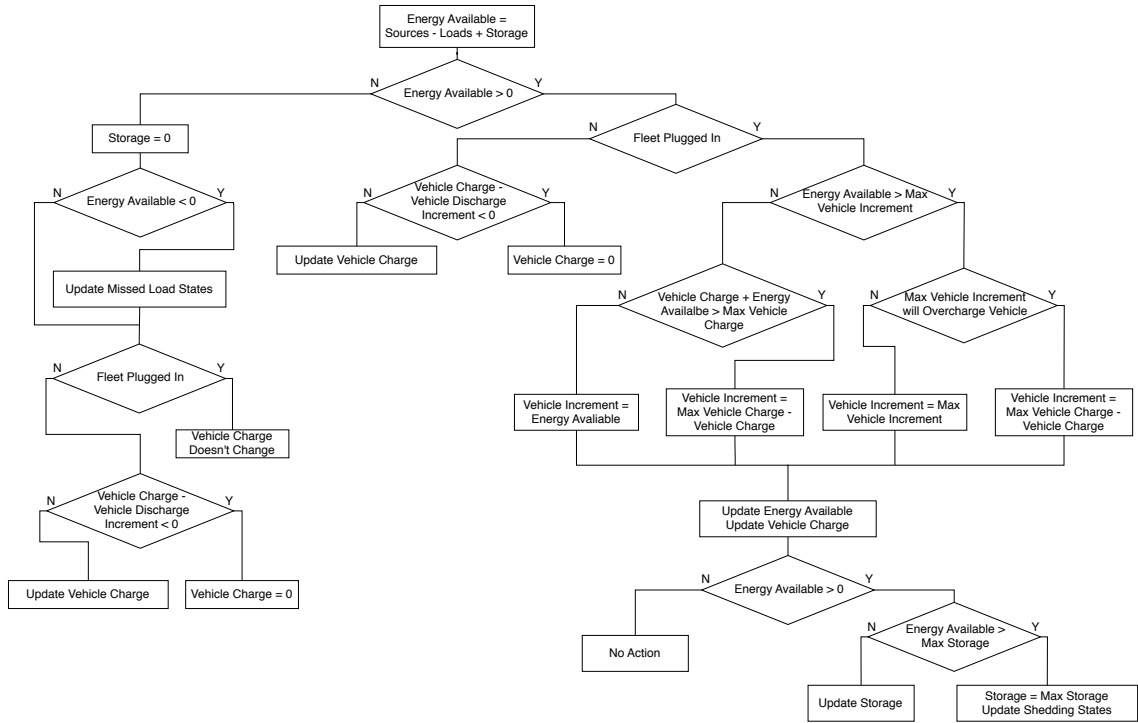


**Figure 2.4:** Simulation flow chart

charge the storage system if it has remaining capacity. If there is no place to put the excess energy, then it is shed.

The model and operational scenario assumptions are summarized as:

1. There are no losses in the grid
2. Energy can flow freely to or from storage as demand necessitates
3. The entire NTV fleet operates as a single unit, either charging or discharging together
4. The NTV fleet is in use and discharging whenever not connected to the grid

A sample storage system and NTV fleet energy state time history is shown in Figure 2.5 for the parameters listed in Table 2.1. At the beginning of the simulation the NTV fleet state of charge decreases at a constant rate since it is not plugged into the grid. The storage system has a relatively low initial charge which depletes in the first 90 minutes, at which time the storage energy remains zero and loads are missed until the PV generation ramps up and can satisfy the primary loads. The storage system charges in-step with the PV source over the day with some extra capacity to charge the NTV fleet when it is plugged in for the day. At about 1400 the storage maximum is reached and there is shed energy for about an hour (demonstrated by the flat top of the Storage Energy curve in Figure 2.5) until PV generation drops. At about 2200 the storage system is once again depleted, but the excess fixed generation allows the NTV fleet to charge, however not back to 100% by the end of the 24 hour period. There is not enough power generated to charge the storage system so its final state is depleted.

### **2.2.2 Analysis**

Using a gradient-based optimization approach (MATLAB's `fmincon` function) in the simulation, the PV array and storage system were sized. Also, the storage system's initial state of charge for a specified number of vehicles in the NTV fleet between 15 and 25 was set. The cost function minimized was the weighted sum of the PV array size and the storage system to reflect the total cost of the system. The constraints, imposed using an additional

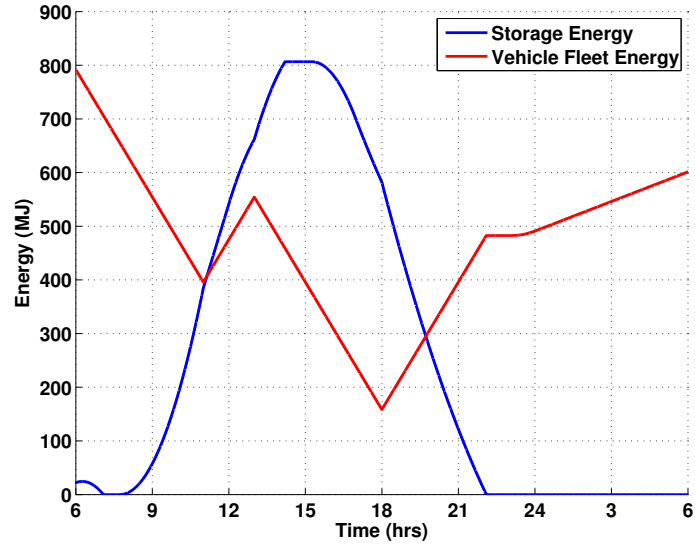


**Figure 2.5:** Storage and NTV fleet energy states for a 20-vehicle grid, not optimized

penalty term in the cost functions, were:

1. The storage system begins and ends the day with the same state of charge,

$$E_{storinit} = E_{storfinal}$$

2. The NTV fleet is fully charged at the end of the day,  $E_{NTVfinal} = 100\%$

3. There are no missed loads,  $E_{missed} = 0$

4. There is no shed energy,  $E_{shed} = 0$

The optimal solution parameters for a grid with a 20 vehicle NTV fleet are shown in Table 2.2, and the storage system and fleet energy state time history are depicted in Figure 2.6. There are three key features to note about the optimized solution in Figure 2.6 when compared to the non-optimal simulation shown in Figure 2.5. First, after about 90 minutes,

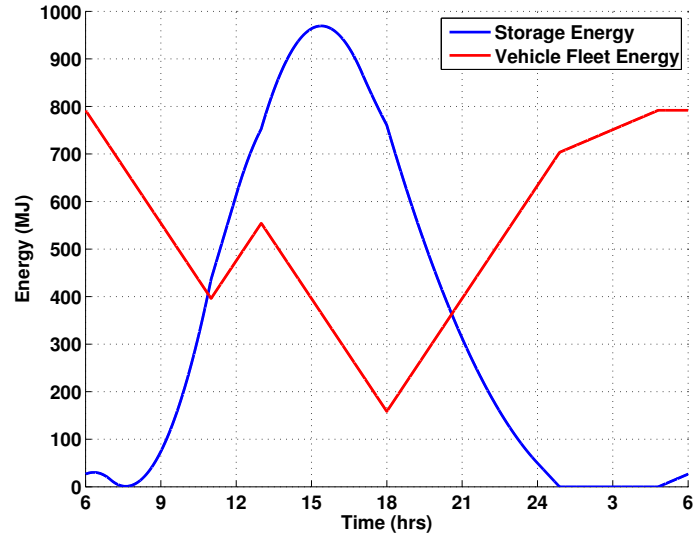


**Figure 2.6:** Storage and NTV fleet energy states for optimized 20-vehicle grid

0730, the storage dips down to zero but the PV generation increases enough at that time to charge the storage supply and avoid any missed loads. Second, when the state of the storage system reaches its peak around 1500, it does not saturate and so there is no shed energy. Third, the storage again dips back to zero toward the end of the day, 0100 to 0500, while the vehicles are charging, but there is enough energy to fully charge the fleet and to replenish the storage supply to its initial state. Also note that although the storage is at zero, there are no missed loads because the NTV fleet is charging at a reduced rate to accommodate the energy state of the system.

**Table 2.2**  
Optimized simulation parameters

| <i>Fleet Size</i> | $P_{PVmax}$ (W) | $E_{stormax}$ (J) | $E_{storinit}$ (J) | <i>Cost</i> |
|-------------------|-----------------|-------------------|--------------------|-------------|
| 15                | 1.004E+05       | 8.866E+08         | 3.714E+07          | 18.908      |
| 16                | 1.013E+05       | 9.038E+08         | 3.574E+07          | 19.173      |
| 17                | 1.022E+05       | 9.191E+08         | 3.245E+07          | 19.416      |
| 18                | 1.032E+05       | 9.355E+08         | 3.024E+07          | 19.672      |
| 19                | 1.041E+05       | 9.519E+08         | 2.790E+07          | 19.927      |
| 20                | 1.050E+05       | 9.693E+08         | 2.659E+07          | 20.194      |
| 21                | 1.059E+05       | 9.850E+08         | 2.349E+07          | 20.442      |
| 22                | 1.068E+05       | 1.002E+09         | 2.140E+07          | 20.701      |
| 23                | 1.077E+05       | 1.019E+09         | 1.960E+07          | 20.964      |
| 24                | 1.087E+05       | 1.036E+09         | 1.734E+07          | 21.222      |
| 25                | 1.096E+05       | 1.053E+09         | 1.617E+07          | 21.775      |

## 2.3 Results

Optimal solutions are found for grids with 15 to 25 vehicle fleets. Table 2.2 and Figure 2.7 show the optimal parameter results for each vehicle case considered. The trends for all three optimization parameters are nearly linear as a function of vehicle number. For all results, the 20-vehicle optimized grid is used as the benchmark to normalize the other results for comparison.

To examine the effect of the fleet size on the grid, each optimal design in Table 2.2 is run through the simulation with 50% PV power reduction to represent a decrease in renewable source output. This resulted in times where the primary loads were missed, and also in reduced NTV fleet state of charge. Figure 2.8 shows the amount of time that primary loads were missed and Figure 2.9 shows the reduction in NTV fleet state of charge at the

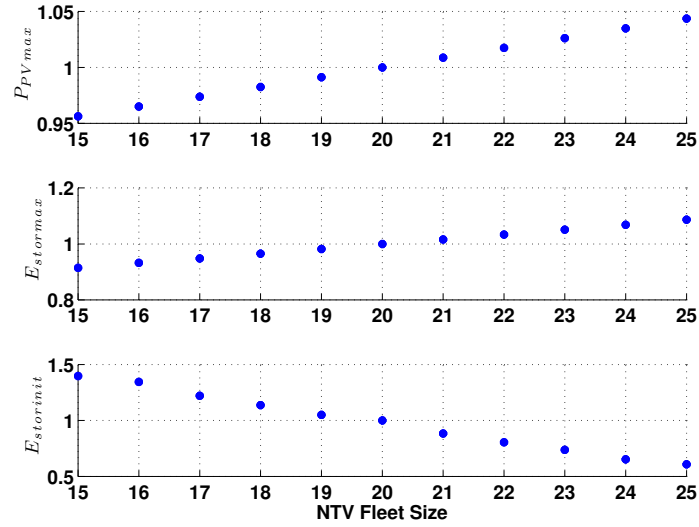


**Figure 2.7:** Optimized simulation parameters normalized to the 20-vehicle grid solution

end of the 24 hour simulation for each optimal solution with 50% PV reduction. As the number of vehicles increases, the amount of missed primary load decreases. This occurs because the primary load size is constant across all vehicle scenarios. As the number of vehicles increases, the generation increases and the percent contribution of the primary loads to the total capacity of the system decreases. Although the missed time at 50% PV output decreases as the NTV fleet size increases, the final energy state of the vehicle fleet decreases with more vehicles because they become a larger fraction of the total load.

## 2.4 Conclusions

The goal of the work in this chapter is to demonstrate that dispatchable NTV loads can be used to stabilize microgrids with high penetration renewable sources, and the results shown

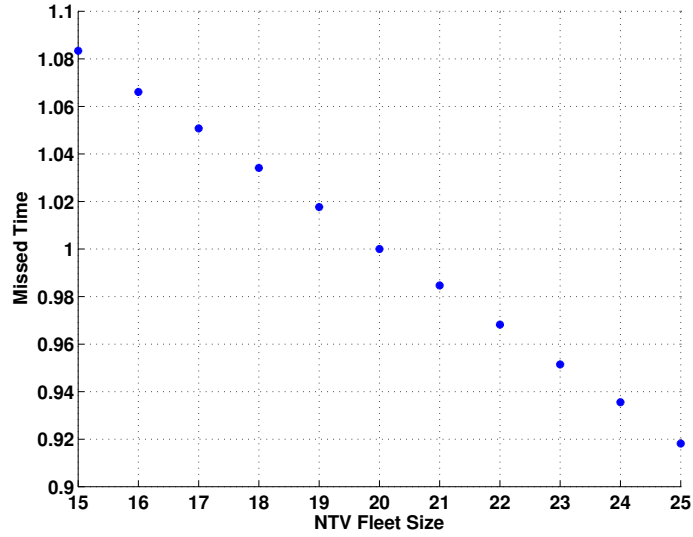


**Figure 2.8:** Missed energy time in optimized grids for 50% loss in PV output normalized to 20-vehicle grid solution, missed time is 36,476 second for 20-vehicle case

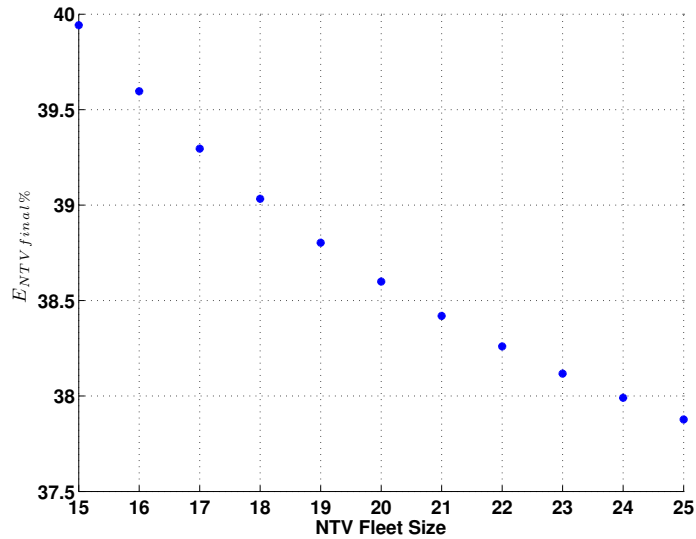


**Figure 2.9:** Vehicle fleet final energy state with 50% PV output

in Figure 2.8 support this claim. Optimizing the grid for a dispatchable fleet decreases the missed energy time from an unpredictable drop in renewable sources. Furthermore, the missed time decreases as the size of the vehicle fleet increases. Thus, for sufficiently large vehicle fleets, all the primary loads can still be met when sources drop. This would be

possible only when the NTV load is at a much higher penetration level than was explored here.

One negative consequence is that the vehicles will not have the desired energy state at the end of the day. Additionally, vehicles will have a lower percentage of their total energy level as the number of vehicles increases. Thus, the findings do demonstrate that there is some relevance in optimal parameter sizing for microgrids with electric vehicles, however it is not the only, and may not be the best, solution for accommodating similar grid architectures.

# Chapter 3

## Distributed Smart Charge Control

### 3.1 Introduction

A smart grid is a power grid with information transfer allowing agents on the grid to communicate and make decisions regarding load connections. One major advantage of a smart grid is the opportunity to more efficiently utilize the power that is generated. When considering a conventional power grid that uses load forecasting to predict power demands, it is possible to account for activities that have been exhibited for many years such as the cycle of the modern family to work or school and back home again. When an additional element outside of the historical forecasted data is added to the power demands it can

---

The material contained in this chapter, including all figures, was previously published as a conference article at the IEEE International Symposium on Power Electronics, Electric Drives, Automation and Motion 2012 with minor changes and additions to adequately fit this text[2].

be difficult to compensate. Such a scenario could present itself with the emergence of plug-in electric vehicles (PEVs). Not only is the additional load associated with PEVs uncertain due to their adoption rate, but it could also prove difficult to quantify because of the stochastic nature of vehicle use. This chapter investigates the use of distributed control of PEV charging on a smart grid allowing for a more manageable overall use of power. The information transfer is used by the PEV's control strategy to make efficient charging decisions.

## **3.2 Methodology**

This section will describe the development of a method to control the charging of PEVs in a smart grid such that the maximum power availability is not exceeded. A simulation was constructed in MATLAB to demonstrate the effect that a smart charging scheme can have on the grid loads.

### **3.2.1 Model Description**

The model can be divided into two main components: the forecasted load profile, and the PEV loads. The size of the grid is based on the city of Houghton, Michigan, which as of the 2010 US Census had a population of 7708 [18]. Static load profiles were obtained

from Southern California Edison for households, small power consumption business firms, medium consumption firms, and large consumption firms [19]. According to census data, the profiles were assembled as follows: 2516 households, 296 small consumption firms, 150 medium consumption firms, and 4 large consumption firms. The individual profiles provided loads at one hour increments over 365 days, which were then averaged over the year to obtain a single, representative day. The profile was interpolated and filtered using the following transfer function to obtain a one second time step:

$$\frac{\text{Filtered Load}}{\text{Raw Load Data}} = \frac{1}{1000s + 1}.$$

The number of PEVs was set to 1000, which is roughly 17% of the total number of vehicles that would be in the area assuming an average of 2.28 vehicles per household [20]. Vehicle use was divided into two equal length segments during the day with starting times normally distributed among the PEVs with mean times of 0830 and 1630 and a standard deviation of 2 hours. This semi-random use schedule is meant to represent the travel to and from work.

The simulation consists of the components described above operating in a simplified smart grid environment. The simplifying assumptions are:

1. There are no losses in the grid.
2. PEVs are in use and discharging at a constant rate when not connected to the grid.

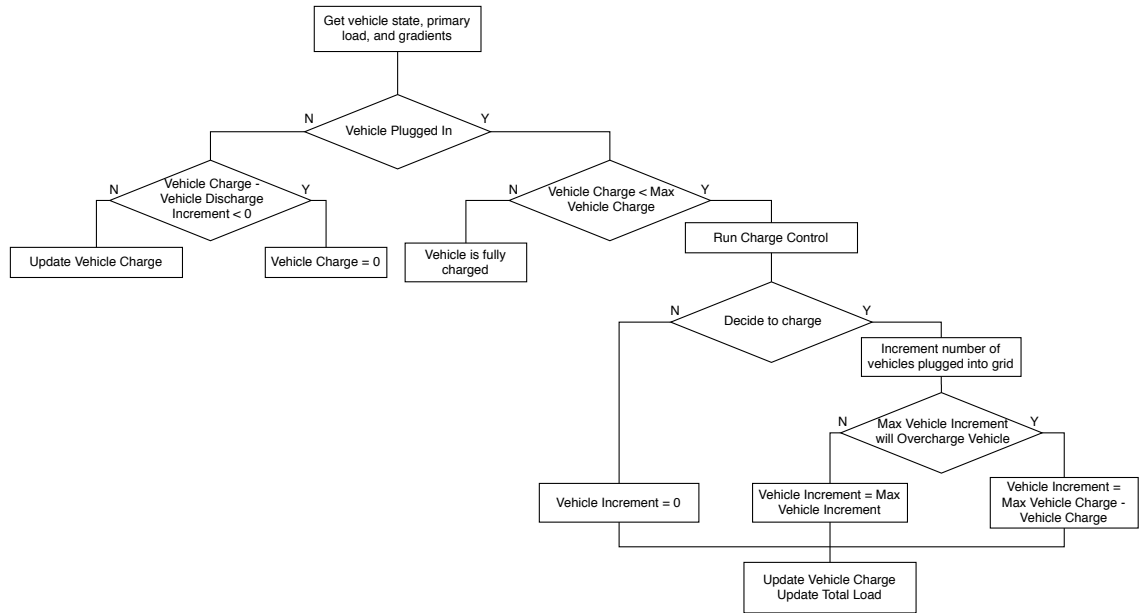


**Figure 3.1:** Simulation flow chart

In this simulation, the non-PEV load is equal to the forecast load described in the previous section and will be referred to as the primary load. When a PEV is plugged into the grid it utilizes the information transfer with the grid to determine if charging at the current time step is acceptable, before applying an additional load to the grid. A flowchart describing the simulation is shown in Figure 3.1.

The baseline strategy operates with no utilization of information transfer and the vehicles charge whenever they are plugged into the grid until they are fully charged. The effect of this strategy on the grid load is shown in Figure 3.2. The primary load profile is shown in black and the addition of the PEVs is blue. The additional load due to the vehicles increases the maximum power demand by 5.9% and increases the overall range by 16.7%.

Initially all the vehicles start the day with a full battery, so there is no additional load at

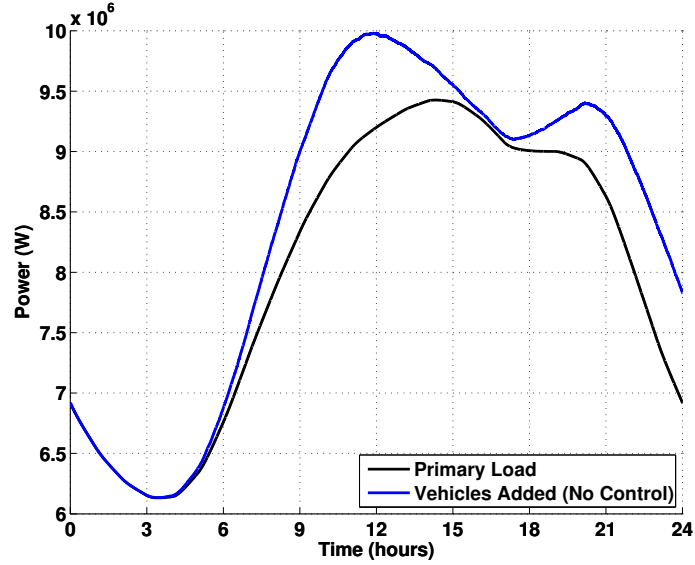


**Figure 3.2:** Load profile for 24-hour period with and without PEV load and no charge control used

the beginning of the day. At the end of the day the vehicles are not fully charged and they continue to charge through the end of 24 hours so the vehicles added load is greater at the end of the day than at the beginning. The vehicles added load with no charge control is less than desirable because it has a significant increase in the amount of power that needs to be supplied. It was previously stated that the maximum load increases by 5.9%, but furthermore at the corresponding new peak the demand is 8.6% higher than the forecasted primary load at that time, about 1100. To negate these negative load effects of the additional PEV load, a smart charging scheme was added so that the vehicles could make a decision to charge and add their load to the grid.

### 3.2.2 Analysis

The goal of the smart charging scheme is to even out the charging and eliminate peaks associated with the PEVs. Moreover, it is desirable to negate both excess loads where there is already a peak due to the primary load and new maxima that would require additional turbines at the power plant. This is done through the use of a charge control algorithm.

At each time step the vehicles interrogate the grid state and then execute their local control algorithm to make a charging decision. The vehicle receives four pieces of information from the grid:

1. The number of vehicles currently charging normalized by the total number of PEVs,

$$\hat{n}_{curr}$$

2. The primary load at that time step normalized by the maximum of the forecasted

$$\text{loads, } \hat{l}_{curr}$$

3. The gradient between the current primary load and the previous primary load,  $\hat{\nabla}_{curr}$

4. The gradient from the previous time step,  $\hat{\nabla}_{prev}$

Using these four values plus the vehicle's current state of charge a decision is made. If the vehicle decides to charge, then its load is added to the primary load and the grid increments the number of vehicles charging. The order in which the vehicles make their decisions is

randomized at each one second time step so that the same vehicles are not always the ones charging.

Using this architecture, many different control algorithms were implemented to find the desired load-leveling behavior described above.

### 3.3 Results

While there were many algorithms tested with varying levels of success as defined by the goals of the study, three will be discussed here. Each algorithm decides on a “cost” associated with the ability to charge that is a function of the information from the grid. If the state of the grid is more receptive to charging the cost will be low. The vehicle determines its own “wealth” as some function of its current state of charge. If the PEV’s wealth is greater than the cost then it will charge for that time step.

The first algorithm discussed will be referred to as Charge Control A. Using the current and previous gradients, Control A determines if the primary load is near a peak, either local or global, and imposes a peak penalty equal to the inverse of the magnitude of the current gradient plus a small constant  $\epsilon$  if a peak is near, otherwise the penalty is zero.

$$P_{peak,A} = \begin{cases} 1/(|\hat{\nabla}_{curr}| + \epsilon) & , \hat{\nabla}_{curr} < \hat{\nabla}_{prev} \\ 0 & , \hat{\nabla}_{curr} \geq \hat{\nabla}_{prev} \end{cases} .$$

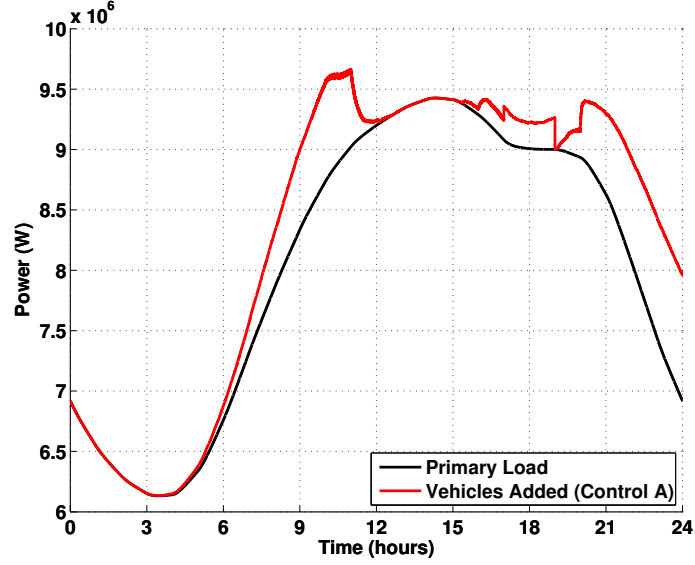


**Figure 3.3:** Load profile for 24-hour time period with and without PEV load using Charge Control B,  $\alpha_w = 3$

The cost determined at each time step,  $C_A$ , is calculated using

$$C_A = p_{peak,A} + \hat{l}_{curr} + \hat{n}_{curr}, \quad (3.1)$$

and the wealth calculated using

$$W_A = \alpha_w / (SOC + \varepsilon), \quad (3.2)$$

where  $\alpha_w$  is a constant multiplier and  $SOC$  is the vehicle's current state of charge as a fraction of its maximum. The results of the simulation using Charge Control A with  $\alpha_w = 3$  can be seen in Figure 3.3. Varying  $\alpha_w$  in Eq. 3.2 will affect the band of time when the vehicles added load matches the primary load in the middle of the day. A smaller multiplier will decrease that band and a larger one will increase it.

Charge Control A reduces the peak due to the PEVs that was exhibited when no control was used. The maximum load with vehicles added is 9.66 MW, which is a 3.2% reduction from no control. While Control A has notable success, the overall load is, at times, discontinuous with immediate changes and large drop offs or spikes in demand. This behavior is undesirable because it is difficult to plan and accommodate for from a generation standpoint. This is driven by the sensitivity of Eq. 3.1 to changes in gradient due to the  $p_{peak,A}$  term.

The second control algorithm will be called Charge Control B. Like Control A, Control B uses the current and previous gradients to detect a peak and apply a penalty. The peak penalty for Control B is equal to the normalized current load,  $\hat{l}_{curr}$ , if near a peak, otherwise it is zero:

$$p_{peak,B} = \begin{cases} \hat{l}_{curr} & , \hat{\nabla}_{curr} < \hat{\nabla}_{prev} \\ 0 & , \hat{\nabla}_{curr} \geq \hat{\nabla}_{prev} \end{cases} .$$

The cost for Control B is calculated with

$$C_B = p_{peak,B} + \hat{n}_{curr} \tag{3.3}$$

and the wealth is calculated with

$$W_B = 2 \cdot (1 - SOC^2). \tag{3.4}$$

Because both terms in Eq. 3.3 are normalized, the maximum cost is two. The wealth, Eq. 3.4, of the vehicle is again a function of the current state of charge, and has a constant multiplier of 2 so that both  $C_B$  and  $W_B$  vary between zero and two. The results of using Charge Control B are shown in Figure 3.4.

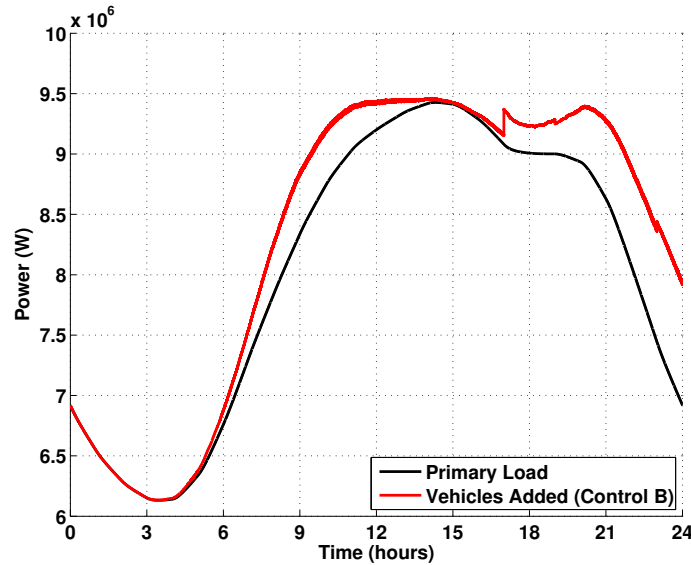


**Figure 3.4:** Load profile for 24-hour time period with and without PEV load using Charge Control B

Control B also successfully reduces the maximum peak exhibited in Figure 3.2. The maximum load using Control B is 9.46 MW, 5.2% less than no control. This is a larger peak reduction than Control A and it is also a smoother profile, which make it a more favorable option than Control A. There are still discontinuities associated with Control B which occur because of the  $p_{peak,B}$  term in Eq. 3.3. At the time of the spikes the algorithm determines that the primary load is switching to or from a peak and the cost to charge at that time significantly changes and either allows or discourages many more PEVs to charge.

The last algorithm, Charge Control C, seeks to eliminate the switching behavior exhibited by Control B. To accomplish this, the peak penalty is dropped from Eq. 3.1 making the cost for Control C

$$C_C = \hat{l}_{curr} + \hat{n}_{curr}. \quad (3.5)$$

The wealth remains the same as with Control B,

$$W_C = W_B = 2 \cdot (1 - SOC^2). \quad (3.6)$$

The results of using Charge Control C are shown in Figure 3.5.

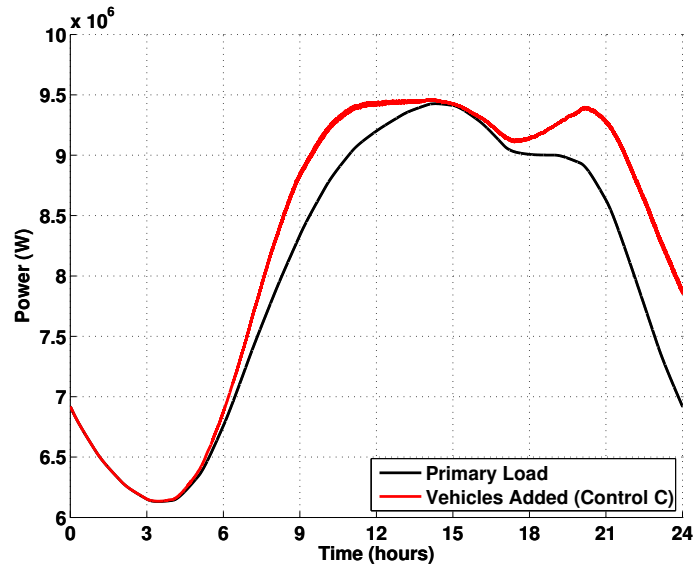


**Figure 3.5:** Load profile for 24-hour time period with and without PEV load using Charge Control C

The maximum load using Control C is the same as while using Control B, for a 5.2% decrease in peak demand from the no control scenario. This occurs because at the primary load peaks the cost for Control B and Control C, Eq. 3.3 and Eq. 3.5 respectively, are the same and the wealth of the vehicle does not change between the controls. The notable difference is that Control C does eliminate the switching exhibited by Control B, which is accomplished by eliminating the peak penalty.

Control C was also used in a six-day simulation, which can be seen in Figure 3.6 where the case of no control is also shown. For both cases with the vehicles added, a noticeable increase in load can be seen from the first to second day. However, after the second day the peaks reach a steady state value, depicted by the dashed lines, and the grid falls into a limit cycle. The controlled load has only a 2.8% increase in its maximum peak over the primary load, whereas the uncontrolled load increases the maximum load by 6.7%.

### **3.4 Conclusions**

The goal of the work in this chapter was to demonstrate that in a smart grid, PEVs could utilize information transfer with the grid to shape the effect exhibited on the overall load. Specifically, charging at peak times can be avoided and large charge induced peaks can be eliminated. This will make it easier to generate the necessary power even when it will be impossible to predict exactly how and when PEVs will be used.

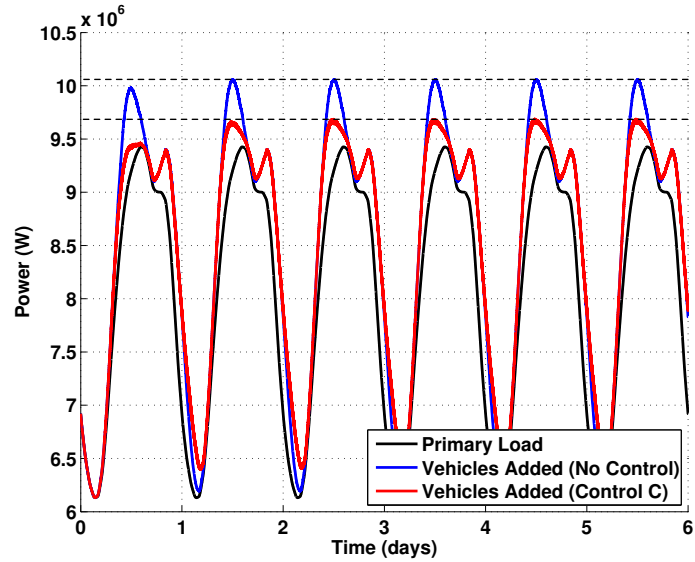


**Figure 3.6:** Load profile for 6-day time period with and without PEV load using no control and Charge Control C

There are, however, some drawbacks to using such a method. On average, the PEV state of charge is lower at the end of the day than it was at the beginning because the charging is restricted. Comparing Figure 3.3, 3.4, or 3.5 to Figure 3.2, the total energy consumption during the day is lower. Because the primary load does not change, it is clear that the vehicles do not obtain the maximum amount of energy.

# **Chapter 4**

## **Discussion**

### **4.1 Summary**

This thesis began with a look into the current state of research in the interaction between plug-in electric vehicles (PEVs) and smart and microgrids. There has been considerable work done in the area of microgrid optimization with renewable sources, but not with the addition of PEVs. Chapter 2 develops a model of a military base microgrid with a 50% penetration of solar photovoltaic (PV) generation. There is also an electrified non-tactical vehicle (NTV) fleet operating on the grid. An optimization scheme is used to size the components of the grid to maximize the efficiency of the generated power. The PV generation is then cut in half to represent an unexpected loss in renewable output. It

is shown that the dispatchable nature of the NTV fleet guards against missed loads in the primary grid, and further that for sufficiently large fleet sizes the primary loads on the grid can be completely unaffected. While the results do provide relevance for the microgrid optimization method presented to stabilize the grid, there are still considerable drawbacks such as a low NTV fleet state of charge following a decrease in renewable generation. There are other options for utilizing PEVs on the grid that may provide more favorable results, such as an intelligent method for charging.

The research surrounding smart charging focuses mainly on optimizing the time of day that vehicles charge and on supervisory control with the grid determining the best charging options. Optimizing the time of day has proven to be an effective method but does not allow for on the fly changes. Supervisory control provides more versatility than time of use but it is computationally expensive for the grid to accomplish for large scenarios. Only a small amount of work has been done in distributed control for PEV charging. Chapter 3 introduces three methods for distributed smart charging of PEVs on a smart grid. Each method is lightweight, requiring only minimal information from the grid, and needs zero user input. The goal was to develop a control algorithm that reduces large peak power demands resulting from the addition of PEV charging loads. Each of the strategies presented does have this effect to varying degrees, but no specific, best control strategy was developed.

## 4.2 Future Work

The findings in Chapter 2 demonstrate that there is some relevance in additionally studying similar microgrid architectures. The work done here could be extended to explore further renewable penetration levels, more diverse grid architecture, and larger NTV fleets among other possible scenarios.

Other future investigations into this subject should consider different renewable sources, as well as real world data. The transient, dynamic behavior of the grid could be incorporated to show the losses in the system and yield a more realistic model as could a different approach to the NTV fleet that tracks the individual vehicles and allows for vehicles to have different use schedules. In addition, these optimization profiles can be used as ideal open-loop profiles and by merging with closed-loop control architecture [21] designs, one can then start to develop robust systems to accommodate the transient behavior and identify more specifically, the storage device dynamic requirements, such as power, energy, and frequency responses.

Another emerging area of research that would fit well into this work is vehicle-to-grid (V2G). V2G explores the use of PEVs as not only dispatchable loads, but also sources with the ability to provide electricity back into the grid. This could prove particularly useful in a microgrid architecture with high penetration renewables. Although significant additional

control strategies may need to be developed, V2G could be used to further stabilize the grid.

While Chapter 3 has proven the relevance of a PEV charge control algorithm, there is still much work that can be done on this subject. The algorithms used here are still untested on other grid configurations and for extended periods of time. While eliminating peak penalty in the cost for Control C did get rid of the switching exhibited by Control B, there still may be some relevance to using a smoother penalty term to encourage charging between peaks. The vehicles charge more between primary load peaks, 1500 to 2000, with Control B, Figure 3.4, than with Control C, Figure 3.5. This happens because the peak penalty term helps to determine that it is a good time to charge. If the penalty was smoothed so that there is not an instantaneous switch, then the vehicle charging would “fill in” between peaks.

As stated previously, the control strategies presented leave at least a portion of the vehicles with a lower state of charge than they started with. New strategies could put more emphasis on the state of the vehicles and not just the state of the grid. One method for doing this would be to incorporate multiple charging levels for the vehicles so that it is possible to charge at different rates.

Another method to accommodate the addition of PEV charging is with the introduction of a high penetration of renewable sources. Consider Figure 3.2 that depicts the primary/forecast grid load and the addition of the vehicles with no control strategy. A large peak develops from the addition of the vehicles at midday. Now consider the source profile

from the microgrid optimization, Figure 2.2. It is a simplified depiction of PV production, but it does follow the general trend of increasing output from sunup until midday and then decreasing output to sundown. Similar trends are exhibited with other renewable sources as well. So, large demand increases occur on a similar time frame to renewable energy output. Instead of limiting the charging of the PEVs through charge control, strategic use of renewable sources could provide for the additional load. With a conventional power plant it is costly to use additional turbines, but that is not necessarily the case with renewables. By using multiple types of renewable sources, the control problem then becomes how best to utilize the renewable sources to meet the energy demands on the grid.

# References

- [1] K. Bordeau, G. Parker, G. Vosters, W. Weaver, D. Wilson, and R. Robinett, “Microgrid modeling and control to investigate the stability impact of hybrid vehicle loads and renewable sources,” in *Proceedings of the NDIA Ground Vehicle Systems Engineering and Technology Symposium, Vehicle Electronics and Architecture (VEA) Mini-Symposium*, Aug. 2011.
- [2] K. Bordeau, G. Parker, G. Vosters, W. Weaver, J. Kelly, D. Wilson, and R. Robinett, “Distributed control of plug-in hybrid electric vehicles on a smart grid,” in *International Symposium on Power Electronics, Electrical Drives, Automation and Motion (SPEEDAM)*, June 2012.
- [3] S. M. Kaplan, “Electric power transmission: Background and policy issues,” tech. rep., Congressional Research Service, April 2009.
- [4] R. Albert, I. Albert, and G. L. Nakarado, “Structural vulnerability of the north american power grid,” *Phys. Rev. E*, vol. 69, Feb 2004.

- [5] U. S. D. of Energy, "'grid 2030" a national vision for electricity's second 100 years," tech. rep., Office of Electric Transmission and Distribution, July 2003.
- [6] N. E. T. Laboratory, "A vision for the smart grid," tech. rep., U.S. Department of Energy Office of Electricity Delivery and Energy Reliability, June 2009.
- [7] S. Amin and B. Wollenberg, "Toward a smart grid: power delivery for the 21st century," *Power and Energy Magazine, IEEE*, vol. 3, no. 5, pp. 34–41, 2005.
- [8] R. Lasseter, "Microgrids," in *Power Engineering Society Winter Meeting, 2002. IEEE*, vol. 1, pp. 305–308 vol.1, 2002.
- [9] R. Lasseter and P. Paigi, "Microgrid: a conceptual solution," in *Power Electronics Specialists Conference, 2004. PESC 04. 2004 IEEE 35th Annual*, vol. 6, pp. 4285–4290 Vol.6, 2004.
- [10] E. Strickland, "A microgrid that wouldn't quit," October 2011.
- [11] R. Chudgar and J. Jennings, "Intelligent automation and controls of power industry microgrid solutions," in *World Automation Congress (WAC), 2012*, 2012.
- [12] U. Reiner, C. Elsinger, and T. Leibfried, "Distributed self organising electric vehicle charge controller system: Peak power demand and grid load reduction with adaptive ev charging stations," in *Electric Vehicle Conference (IEVC), 2012 IEEE International*, pp. 1–6, 2012.

- [13] R. A. Waraich, M. D. Galus, C. Dobler, M. Balmer, G. Andersson, and K. W. Axhausen, "Plug-in hybrid electric vehicles and smart grids: Investigations based on a microsimulation," *Transportation Research Part C: Emerging Technologies*, vol. 28, pp. 74 – 86, 2013.
- [14] A. Halbleib, M. Turner, and J. Naber, "Control of battery electric vehicle charging for commercial time of day demand rate payers," in *Innovative Smart Grid Technologies (ISGT), 2012 IEEE PES*, pp. 1–5, 2012.
- [15] D. Halamay and et al., "Reserve requirement impacts of large-scale integration of wind, solar, and ocean wave power generation," *IEEE Transactions on Sustainable Energy*, vol. 2, pp. 321–328, 2011.
- [16] J. Ehnberg and M. Bollen, "Generation reliability for small isolated power systems entirely based on renewable sources," in *IEEE Power Engineering Society General Meeting*, pp. 2322–2327, 2004.
- [17] W. Lachs and et al., "Power system control in the next century," *IEEE Transactions on Power Systems*, vol. 11, pp. 11–18, 1996.
- [18] U. C. Bureau, "Houghton (city) quickfacts from the us census bureau." <http://quickfacts.census.gov/qfd/states/26/2639360.html>, January 2012.

- [19] S. C. Edison, “Sce-2011 static load profiles.” <http://www.sce.com/AboutSCE/Regulatory/loadprofiles/2011loadprofiles.htm>, 2012.
- [20] A. A. News, “Study finds americans own 2.28 vehicles per household.” <http://www.autospies.com/news/Study-Finds-Americans-Own-2-28-Vehicles-Per-Household-26437/>, February 2008.
- [21] R. R. III and D. Wilson, *Nonlinear Power Flow Control: Utilizing Exergy, Entropy, Static and Dynamic Stability, and Lyapunov Analysis*, ch. Chapter 10. 2011.
- [22] W. Weaver, “Dynamic energy resource control of power electronics in local area power networks,” *IEEE Transactions on Power Electronics*, vol. 26, pp. 852–859, March 2011.
- [23] W. Weaver and P. Krein, “Game-theoretic control of small-scale power systems,” *IEEE Transactions on Power Delivery*, vol. 24, pp. 1560–1567, July 2009.
- [24] W. Weaver, C. Anderson, J. Naber, J. Keith, J. Worm, J. Beard, B. Chen, and S. Hackney, “An interdisciplinary program for education and outreach in hybrid-electric drive vehicle engineering at michigan technological university,” in *IEEE Vehicle Power and Propulsion Conference*, vol. 1, pp. 1–6, sept. 2011.
- [25] M. J. Tatro, J. M. Covan, R. Robinett, G. W. Kuswa, D. Menicucci, and S. A. Jones, “Toward an energy surety future,” Sandia Report SAND2005-6281, Oct. 2005.

- [26] R. D. Robinett III and D. G. Wilson, *Nonlinear Power Flow Control Design: Utilizing Exergy, Entropy, Static and Dynamic Stability, and Lyapunov Analysis*. Springer-Verlag, 2011.
- [27] J. Davis and et al., “Multi-domain surety modeling and analysis for high assurance systems,” in *IEEE Conference and Workshop on Engineering of Computer-Based Systems*, pp. 254–260, 1999.
- [28] W. Kempton and J. Tomic, “Vehicle-to-grid power implementation: From stabilizing the grid to supporting large-scale renewable energy,” *Journal of Power Sources*, vol. 144, pp. 208–294, 2005.

# Appendix A

## MATLAB Code

The code to accomplish the microgrid optimization process is divided into three pieces: a setup script, an optimization function script, and a grid simulation function. The setup script loads necessary data as well as initializing variables and parameters that will be used and calls MATLAB's `fmincon` function. `fmincon` then calls the optimization function script that simulates the microgrid with the grid simulation function and then calculates the cost function. `fmincon` uses the cost function from each simulated grid day and determines new grid parameters until an optimal grid solution is found.

# A.1 Microgrid Component Optimal Sizing Code

## A.1.1 Setup Script

```
NPTS = 86401;
DT = 1.0;

format long

% Each vehicle as an 11kW-hr capacity ,
% or 11,000*3600 = 39.6 MJ. This is roughly a Chevy Volt. The Volt is
% claimed to charge in 10-12 hours at 120V and 3 hours at 240V.
% Based on the charge time above, the rate of charge is:
% 39.6MJ/(10*3600)s = 1100 J/s. At the start of the day (5AM) the
% fleet must have a nominal charge that is larger than some required
% minimum.
% FLEETSIZE = 20;
% MAXVEHCHARGE = 39.6E6; % (J)
% MAXVEHCHARGERATE = 1100; % (J/s)
% NOMINALVEHFULLCHARGERATIO = 0.8; % (n.d.)

%XVIC = 1; % params index for vehicle charge IC
%XCIC = 2; % params index for storage system IC

%fleetinitcharge = MAXVEHCHARGE * FLEETSIZE * NOMINALFULLCHARGE;

%*****
%*** OPTIMIZATION PARAMETERS
%*****

% Here's the initial guess
SMAXPWR = 0.11E6; % PV max output (W)
CMAX = 10.0E8; % Storage capacity (J)
CIC = 1.0E8; % Storage initial state (J)
GPWR = 0.05E6; % Generator, constant source power (W)

% The optimization constraints will be:
% 1. CIC(T) = CIC(0)
% 2. vehicle charge @ T = full
% 3. upper and lower bounds on optimization variables

% The cost is $$
% J = SMAXPWR*PVCOST + CMAX*CCOST + GPWR*GCOST
```

```

global optnrm params spwr lpwr plug
global cnrg vnrg shednrg mnrg metrics
global time sol

```

```

%*****
%*** MAKE PV POWER TIME HISTORY
%*****

```

```

spwr = zeros(NPTS,1);
T0 = (6-6)*3600;
T1 = (11-6)*3600;
T2 = (12-6)*3600;
T3 = (17-6)*3600;
AMP = 1;
slopeup = AMP/(T1-T0);
slopedn = -AMP/(T3-T2);
for i=1:NPTS
    if (i > T3)
        spwr(i) = 0;
    elseif (i > T2)
        spwr(i) = slopedn * (i - T3);
    elseif (i > T1)
        spwr(i) = AMP;
    elseif (i > T0)
        spwr(i) = slopeup * (i - T0);
    else
        spwr(i) = 0;
    end;
end;
clear T0 T1 T2 T3 AMP slopeup slopedn i

```

```

%*****
%*** MAKE LOAD POWER TIME HISTORY
%*****

```

```

lpwr = zeros(NPTS,1);
T0 = (6-6)*3600;
T1 = (7-6)*3600;
T2 = (17-6)*3600;
T3 = (24-6)*3600;
AMP = 40000;
slopeup = AMP/(T1-T0);
slopedn = -AMP/(T3-T2);
for i=1:NPTS
    if (i > T3)
        lpwr(i) = 0;
    elseif (i > T2)
        lpwr(i) = slopedn * (i - T3);
    elseif (i > T1)
        lpwr(i) = AMP;
    elseif (i > T0)

```

```

        lpwr(i) = slopeup * (i - T0);
    else
        lpwr(i) = 0;
    end;
end;
end;
T0 = (6-6)*3600;
T1 = (11-6)*3600;
T2 = (13-6)*3600;
AMP = 10000;
clear T0 T1 T2 T3 AMP slopeup slopedn i
lpwr = lpwr + 0.02E6;

%*****
%*** MAKE PLUGGED-IN TIME HISTORY
%*****
plug = zeros(NPTS,1);
T0 = (6-6)*3600;
T1 = (8-6)*3600;
T2 = (11-6)*3600;
T3 = (13-6)*3600;
T4 = (18-6)*3600;
T5 = (21-6)*3600;

for i=1:NPTS
    if (i > T5)
        plug(i) = 1;
    elseif (i > T4)
        plug(i) = 1;
    elseif (i > T3)
        plug(i) = 0;
    elseif (i > T2)
        plug(i) = 1;
    elseif (i > T1)
        plug(i) = 0;
    elseif (i > T0)
        plug(i) = 0;
    else
        plug(i) = 1;
    end;
end;
clear T0 T1 T2 T3 T4 T5 i

params = zeros(5,1);
optnrm = zeros(4,1);
x0 = ones(size(optnrm));

optnrm(1) = SMAXPWR;
optnrm(2) = CMAX;
optnrm(3) = CIC;
optnrm(4) = GPWR;

```

```

FLEETSIZE = 25;
MAXVEHCHARGE = 39.6E6; % (J)
MAXVEHCHARGERATE = 1100; % (J/s)
NOMINALVEHFULLCHARGERATIO = 1.0; % (n.d.)

vuse = 0;
for i=1:NPTS
    vuse = vuse + DT*(1-plug(i));
end;
VNRGUSERATE = FLEETSIZE*NOMINALVEHFULLCHARGERATIO*MAXVEHCHARGE/vuse;

params(1) = FLEETSIZE;
params(2) = MAXVEHCHARGE;
params(3) = MAXVEHCHARGERATE;
params(4) = NOMINALVEHFULLCHARGERATIO;
params(5) = VNRGUSERATE;

time = 0:NPTS-1;

LB = [0.1;0.1;0.1;0.5];
UB = [1.5;1.5;1.7;1.5];

xx = fmincon(@wrapcost,x0,[],[],[],[],LB,UB);
beep

```

## A.1.2 Optimization Function

```

function [J] = wrapcost(x)

global optnrm params spwr lpwr plug
global cnrg vnrg shednrg mnrg metrics
global time simparams h

simparams = zeros(9,1);

simparams(1) = optnrm(1) * x(1); % pv system capacity (W)
simparams(2) = optnrm(2) * x(2); % storage system capacity (J)
simparams(3) = optnrm(3) * x(3); % initial storage state (J)

simparams(4) = 6*simparams(1)*3600/86400;

%%% VERY DANGEROUS
% simparams(1) = simparams(1)*.5;

simparams(5) = params(1); % fleet size (#)

```

```

simparams(6) = params(2);           % max single veh charge (J)
simparams(7) = params(3);           % max single veh charge rate (J/s)
simparams(8) = params(4);           % nominal veh full charge ratio (n.d.)
simparams(9) = params(5);           % veh fleet nrg use rate (J/s)

%[cnrg ,vnrg ,metrics] = nrgsimA(simparams ,spwr ,lpwr ,plug);
[cnrg ,vnrg ,shednrg ,mnrng ,metrics] = nrgsimB(simparams ,spwr ,lpwr ,plug);

%J = metrics(2);

ceq(1) = (cnrg(end) - simparams(3))/(3e7);
ceq(2) = (vnrg(end) - simparams(8)*simparams(6)*simparams(5))/7e8;
%ceq(3) = abs(simparams(4) - 6*simparams(1)*3600/86400);

J = 10*simparams(1)*1e-5 + 10*simparams(2)*1e-9 + ...
    1000*abs(ceq(1)) + 1000*abs(ceq(2)) + ...
    metrics(2)*10000 + sum(shednrg)/1e4;

%J = (simparams(1)*5 + simparams(2)*4 + simparams(4)*7)*1e-8;

[x' J]

spwrTot = simparams(4)+spwr*simparams(1);

set(h(1).plt(1), 'XData', time/3600, 'YData', cnrg);
set(h(1).plt(2), 'XData', time/3600, 'YData', vnrg);
set(h(2).plt(1), 'XData', time/3600, 'YData', mnrng);
set(h(2).plt(2), 'XData', time/3600, 'YData', shednrg);
set(h(3).plt(1), 'XData', time/3600, 'YData', spwrTot);
set(h(3).plt(2), 'XData', time/3600, 'YData', lpwr);
set(h(3).plt(3), 'XData', time/3600, 'YData', plug*1E4);

```

### A.1.3 Grid Simulation Function

```

#include "stdio.h"
#include "math.h"
#include "mex.h"

#define NPTS 86401
#define DT 1.0

void nrgsim(double *simparams ,
            double *spwr ,
            double *lpwr ,

```

```

        double *plug ,
        double *cnrg ,
        double *vnrg ,
        double *shednrg ,
        double *mnrg ,
        double *metrics)
{
    int i;
    double t;

    double vnrginc;
    double nrgavailable;
    double vnrgincmax;
    double fleetsize;
    double maxvehcharge;
    double maxvehchargerate;
    double nominalvehfullchargeratio;
    double smaxpwr, gpwr;
    double cmax, vmax;
    double cic;
    //double shednrg      = 0.0;
    double shedtime      = 0.0;
    //double missednrg    = 0.0;
    double missedtime    = 0.0;
    double vnrguserate   = 0.0;

    smaxpwr                = simparams [0];
    cmax                    = simparams [1];
    cic                     = simparams [2];
    gpwr                    = simparams [3];
    fleetsize               = simparams [4];
    maxvehcharge            = simparams [5];
    maxvehchargerate       = simparams [6];
    nominalvehfullchargeratio = simparams [7];
    vnrguserate             = simparams [8];

    cnrg[0] = cic;
    vnrg[0] = nominalvehfullchargeratio * maxvehcharge * fleetsize;
    shednrg[0] = 0.0;
    mnrg[0] = 0.0;

    vnrgincmax = fleetsize * maxvehchargerate;
    vmax       = fleetsize * maxvehcharge;

    for(i=1;i<NPTS;i++) {
        vnrginc = 0.0;
        nrgavailable = (gpwr+smaxpwr*spwr[i-1]-lpwr[i-1])*DT+cnrg[i-1];
        if(nrgavailable > 0.0) {
            if(plug[i-1] > 0.5) {
                if(nrgavailable > vnrgincmax) {
                    if(vnrg[i-1] + vnrgincmax > vmax) {

```

```

        vnrnginc = vmax - vnrng[i-1]*plug[i-1];
    }
    else
        vnrnginc = vnrngincmax;
}
else {
    if(vnrng[i-1] + nrgavailable > vmax)
        vnrnginc = vmax - vnrng[i-1]*plug[i-1];
    else
        vnrnginc = nrgavailable;
}
nrgavailable -= vnrnginc;
vnrng[i] = vnrng[i-1] + vnrnginc;
}

else
    vnrng[i] = vnrng[i-1] - vnrnguserate*DT;

if(nrgavailable > 0.0) {
    if(nrgavailable > cmax){
        cnrg[i] = cmax;
        shednrg[i]= (nrgavailable - cmax);
        shedtime += DT;
    }
    else
        cnrg[i] = nrgavailable;
}
}
else {
    if(nrgavailable < 0.0) {
        if(plug[i-1] > 0.5) {
            cnrg[i] = 0.0;
            vnrng[i] = vnrng[i-1];
            mnrng[i] = -nrgavailable;
            missedtime += DT;
        }
        else {
            if(vnrng[i-1] - vnrnguserate*DT < 0.0) {
                cnrg[i] = 0.0;
                vnrng[i] = 0.0;
                mnrng[i] = -nrgavailable;
                missedtime += DT;
            }
            else {
                cnrg[i] = 0.0;
                vnrng[i] = vnrng[i-1] - vnrnguserate*DT;
                mnrng[i] = -nrgavailable;
                missedtime += DT;
            }
        }
    }
}
}

```

```

        else {
            if(plug[i-1] > 0.5) {
                cnrg[i] = 0.0;
                vnrg[i] = vnrg[i-1];
            }
            else {
                if(vnrg[i-1] - vnrguserate*DT < 0.0) {
                    cnrg[i] = 0.0;
                    vnrg[i] = 0.0;
                }
                else {
                    cnrg[i] = 0.0;
                    vnrg[i] = vnrg[i-1] - vnrguserate*DT;
                }
            }
        }
    }
}
// metrics[0] = shednrg;
metrics[0] = shedtime;
// metrics[2] = missednrg;
metrics[1] = missedtime;
}

// *****
// *** MEX FUNCTION HANDLER
// *****

void mexFunction( int nlhs , mxArray *plhs[] ,
                 int nrhs , const mxArray *prhs[] )
{
    double *simparams;
    double *spwr;
    double *lpwr;
    double *plug;

    double *cnrg;
    double *vnrg;
    double *shednrg;
    double *mnrng;
    double *metrics;

    /* create matrices for return */
    plhs[0] = mxCreateDoubleMatrix(NPTS,1,mxREAL);
    plhs[1] = mxCreateDoubleMatrix(NPTS,1,mxREAL);
    plhs[2] = mxCreateDoubleMatrix(NPTS,1,mxREAL);
    plhs[3] = mxCreateDoubleMatrix(NPTS,1,mxREAL);
    plhs[4] = mxCreateDoubleMatrix(2,1,mxREAL);

    simparams = mxGetPr(prhs[0]);
    spwr      = mxGetPr(prhs[1]);

```

```

lpwr      = mxGetPr(prhs [2]);
plug      = mxGetPr(prhs [3]);

cnrg      = mxGetPr(plhs [0]);
vnrg      = mxGetPr(plhs [1]);
shednrg   = mxGetPr(plhs [2]);
mnrg      = mxGetPr(plhs [3]);
metrics   = mxGetPr(plhs [4]);

nrgsim(simparams , spwr , lpwr , plug , cnrg , vnrg , shednrg , mnrg , metrics );
}

```

## A.2 Distributed Smart Charge Control Code

The code to accomplish the distributed smart charge control is divided into three pieces: a setup script, a grid simulation function, and a charge control function. The setup script loads necessary data as well as initializing variables and parameters that will be used and calls the grid simulation function. The grid simulation function performs the bulk of the model simulation and keeps track of the PEV battery charges as well as overall grid loads. The charge control function is called by the grid simulation function to determine if a vehicle will charge at a specific time step. There are three charge control functions presented here, one for each of the strategies described in Chapter 3.

### A.2.1 Setup Script

```

tic
clear
NPTS = round(86401/1);

```

```

DT = 1.0;

format long

s = RandStream('mt19937ar','Seed',542);
RandStream.setDefaultStream(s);
% rng(542); % seed random number generator

global params

load('LoadsGrads');
numberHomes = 2516;
numberVehicles = round(2.28*numberHomes);
FLEETSIZE = 1000;
DAYS = 1;

% Each vehicle has an 11kW-hr capacity ,
% or 11,000*3600 = 39.6 MJ. This is roughly a Chevy Volt. The Volt is
% claimed to charge in 10-12 hours at 120V and 3 hours at 240V.
% Based on the charge time above, the rate of charge is:
% 39.6MJ/(10*3600)s = 1100 J/s. At the start of the day (5AM) the
% fleet must have a nominal charge that is larger than some required
% minimum.
% FLEETSIZE = 20;
% MAXVEHCHARGE = 39.6E6; % (J)
% MAXVEHCHARGERATE = 1100; % (J/s)
% NOMINALVEHFULLCHARGERATIO = 0.8; % (n.d.)

%XVIC = 1; % params index for vehicle charge IC
%XCIC = 2; % params index for storage system IC

%fleetinitcharge = MAXVEHCHARGE * FLEETSIZE * NOMINALFULLCHARGE;

%*****
%*** MAKE LOAD POWER TIME HISTORY
% Assembled from information by Southern California Edison
% (http://www.sce.com/AboutSCE/Regulatory/loadprofiles/
% 2011loadprofiles.htm)
% Based on 2010 Houghton, MI census data: 2516 homes, 296 small
% business, 150 medium business, 4 large business (450 total firms).
% Load data provided each hour over 365 days, load was interpolated
% for each second. Loaded from Loads.mat, containing only lpwr.
%*****

lpwr = temp2(:,2)*1e3;
grad = temp2(:,3)*1e3;
MAXGRADIENT = max(abs(grad));

```

```

clear temp2 temp3 temp4
%*****
%*** MAKE PLUGGED-IN TIME HISTORY
%*****

plug = zeros(FLEETSIZE, NPTS);

%*****
for v = 1:FLEETSIZE
    T1 = normrnd(3.5, 2);
    T2 = T1 + 5;
    T3 = normrnd(15.5, 2);
    T4 = T3 + 5;
    T1 = T1*3600;
    T2 = T2*3600;
    T3 = T3*3600;
    T4 = T4*3600;
    for i=1:NPTS
        if (i > T4)
            plug(v, i) = 1;
        elseif (i > T3)
            plug(v, i) = 0;
        elseif (i > T2)
            plug(v, i) = 1;
        elseif (i > T1)
            plug(v, i) = 0;
        else
            plug(v, i) = 1;
        end;
    end;

end;
%*****
%%

clear T0 T1 T2 T3 T4 T5 i

params = zeros(5, 1);

MAXVEHCHARGE = 39.6E6; % (J)
MAXVEHCHARGERATE = 1100; % (J/s)
NOMINALVEHFULLCHARGERATIO = 1.0; % (n.d.)

VNRGUSERATE = 1100; % (J/s)

params(1) = FLEETSIZE;
params(2) = MAXVEHCHARGE;
params(3) = MAXVEHCHARGERATE;
params(4) = NOMINALVEHFULLCHARGERATIO;
params(5) = VNRGUSERATE;
params(6) = DAYS;

```

```

params(7) = MAXGRADIENT;

time = 0:NPTS-1;
time2 = 0:NPTS*DAYS-1;

%*****
%*** CREATE PLOT HANDLES FOR UPDATE
%*****
yy = time;

h(3).fig = figure(2);
clf
h(3).axs = axes;
h(3).plt(1) = line(time,yy);
h(3).plt(2) = line(time,yy);
set(h(3).plt,'LineWidth',2);
set(h(3).plt(1),'Color','b');
set(h(3).plt(2),'Color','g');
set(h(3).axs,'FontSize',14,'FontWeight','Bold');
h(3).xlb = xlabel('Time (hrs)');
h(3).ylb = ylabel('Power (W)');
grid on
h(3).leg = legend('Original Load','Vehicles Added');

clear yy

[lpwrTot,vnrg] = nrgsim(lpwr,plug,grad);

%%
lpwrPlot = zeros(NPTS*DAYS,1);
lpwrPlot(1:NPTS) = lpwr;
for i = 1:DAYS-1
    lpwrPlot(NPTS*i+1:NPTS*(i+1)) = lpwr;
end

set(h(3).plt(1),'XData',time2/3600,'YData',lpwrPlot);
set(h(3).plt(2),'XData',time2/3600,'YData',lpwrTot);
%%
toc

```

## A.2.2 Grid Simulation Function

```

function [lpwrTot,vnrgTot] = nrgsim(lpwr,plug,grad)

```

```

global params

NPTS = 86401;
DT = 1;
PLUGGED = 1;
DISCHARGE = 0;

fleetsize = params(1);
maxvehcharge = params(2);
maxvehchargerate = params(3);
nominalvehfullchargeratio = params(4);
vnrguserate = params(5);
days = params(6);
maxGrad = params(7);

vnrgincmax = maxvehchargerate;
vmax = maxvehcharge;

vnrg = zeros(fleetsize,1);
vnrg(:) = nominalvehfullchargeratio * maxvehcharge;

vnrgTot = zeros(NPTS*days,1);
lpwrTot = zeros(NPTS*days,1);

Nlpwr = lpwr - min(lpwr);

for d = 1:days
    for i = 1:NPTS
        vpwr = 0;
        plugTotal = 0;
        currentLoad = Nlpwr(i)/max(Nlpwr);
        currentGrad = grad(i)/maxGrad;
        if i == 1
            prevGrad = grad(end)/maxGrad;
        else
            prevGrad = grad(i-1)/maxGrad;
        end

        p = randperm(fleetsize);
        for v = 1:fleetsize
            vnrginc = 0;
            veh = p(v);
            switch plug(veh,i)

                case PLUGGED
                    if vnrg(veh) < vmax
                        isCharging = chargeControl_A(plugTotal, currentLoad, ...
                            currentGrad, prevGrad, vrgn(veh));
                    end
            end
        end
    end

```

```

    if isCharging
        plugTotal = plugTotal+1/fleetsize;
        if vnrg(veh) + vnrgincmax > vmax
            vnrginc = vmax - vnrg(veh);
        else
            vnrginc = vnrgincmax;
        end
    end
    vnrg(veh) = vnrg(veh) + vnrginc;

case DISCHARGE
    if vnrg(veh) - vnrguserate*DT < 0
        vnrg(veh) = 0;
    else
        vnrg(veh) = vnrg(veh) - vnrguserate*DT;
    end
end
vpwr = vpwr + vnrginc;
end
curr = i + (d-1)*NPTS;
vnrgTot(curr) = sum(vnrg);
lpwrTot(curr) = lpwr(i) + vpwr;
end
end

```

## A.2.3 Charge Control Functions

### A.2.3.1 Charge Control A

```

function [yesNo] = chargeControl_A(plugTotal ,currentLoad ,...
    currentGrad ,prevGrad ,vnrg)

global params

yesNo = 0;
maxvehcharge = params(2);

cost = currentLoad + plugTotal;
wealth = 2*vnrg/maxvehcharge;

if wealth >= cost
    yesNo = 1;
end

```

### A.2.3.2 Charge Control B

```
function [yesNo] = chargeControl_B(plugTotal ,currentLoad ,...
    currentGrad ,prevGrad ,vnrg)

global params

yesNo = 0;
maxvehcharge = params(2);

if currentGrad < prevGrad
%     disp('PEAK')
    peakPenalty = 1/(abs(currentGrad) + eps);
else
%     disp('TROUGH')
    peakPenalty = 0;
end

alpha = 3;
cost = peakPenalty + currentLoad + plugTotal;
wealth = alpha / (vnrg / maxvehcharge + eps);

if wealth >= cost
    yesNo = 1;
end
```

### A.2.3.3 Charge Control C

```
function [yesNo] = chargeControl_C(plugTotal ,currentLoad ,...
    currentGrad ,prevGrad ,vnrg)

global params

yesNo = 0;
maxvehcharge = params(2);

if currentGrad < prevGrad
%     disp('PEAK')
    peakPenalty = currentLoad;
else
%     disp('TROUGH')
    peakPenalty = 0;
end
```

```
cost = peakPenalty + plugTotal;  
wealth = 2*(1 - (vnrg/maxvehcharge)^2);  
  
if wealth >= cost  
    yesNo = 1;  
end
```

# Appendix B

## Letters of Permission

### B.1 Chapter 2 Permission

A large part of this chapter comes from *Microgrid Modeling and Control to Investigate the Stability Impact of Hybrid Vehicle Loads and Renewable Sources* presented at Ground Vehicle Systems Engineering and Technology Symposium (GVSETS) 2011. The following is an email correspondence with the event contact Chuck Prikopa.

Kyle,

As long as you only reference your paper, we have no problems at all assuming at some point you reference GVSETS in your footnotes. Best of luck on your thesis.

Chuck Prikopa BAE Systems 586-588-0749

—Original Message— From: Kyle Bordeau [mailto:kdbordea@mtu.edu] Sent: Tuesday, March 12, 2013 12:14 PM To: gvsets@ndia-mich.org Subject: Conference paper permissions

I presented a paper that I wrote at the 2011 GVSETS VEA mini-sym. I am now writing my thesis and would like to make sure that I have the proper permission to use material from that paper. Please let me know what I would need to do for this. Thank you.

– Kyle Bordeau MS Student - Mechanical Engineering Michigan Technological University  
kdbordea@mtu.edu

## **B.2 Chapter 3 Permission**

A large part of this chapter comes from *Distributed Control of Plug-in Hybrid Electric Vehicles on a Smart Grid* presented the IEEE International Symposium on Power Electronics, Electrical Drives, Automation and Motion 2012. The following is a statement for reusing IEEE copyright material in a thesis.

Thesis / Dissertation Reuse

The IEEE does not require individuals working on a thesis to obtain a formal reuse license, however, you may print out this statement to be used as a permission grant:

Requirements to be followed when using any portion (e.g., figure, graph, table, or textual material) of an IEEE copyrighted paper in a thesis:

- 1) In the case of textual material (e.g., using short quotes or referring to the work within these papers) users must give full credit to the original source (author, paper, publication) followed by the IEEE copyright line ©2011 IEEE.
- 2) In the case of illustrations or tabular material, we require that the copyright line ©[Year

of original publication] IEEE appear prominently with each reprinted figure and/or table.

- 3) If a substantial portion of the original paper is to be used, and if you are not the senior author, also obtain the senior author's approval.

Requirements to be followed when using an entire IEEE copyrighted paper in a thesis:

- 1) The following IEEE copyright/ credit notice should be placed prominently in the references: ©[year of original publication] IEEE. Reprinted, with permission, from [author names, paper title, IEEE publication title, and month/year of publication]
- 2) Only the accepted version of an IEEE copyrighted paper can be used when posting the paper or your thesis on-line.
- 3) In placing the thesis on the author's university website, please display the following message in a prominent place on the website: In reference to IEEE copyrighted material which is used with permission in this thesis, the IEEE does not endorse any of [university/educational entity's name goes here]'s products or services. Internal or personal use of this material is permitted. If interested in reprinting/republishing IEEE copyrighted material for advertising or promotional purposes or for creating new collective works for resale or redistribution, please go to [http://www.ieee.org/publications\\_standards/publications/rights/rights\\_link.html](http://www.ieee.org/publications_standards/publications/rights/rights_link.html) to learn how to obtain a License from RightsLink.